International Journal of Research in Advent Technology, Vol.6, No.10, October 2018
E-ISSN: 2321-9637
Available online at www.ijrat.org

Molecular Energy Distribution Studies on Dyes Doped KDP Crystals for Laser Applications

S.Rajesh kumar[1]*, P.Kumaresan[2]
[1]*P.G Department of physics, King Nandhivarman College of Arts and Science, Thellar-604406, Tamil Nadu, India.
[2] P.G & Research Department of Physics, Thiru.A.Govindasamy Government Arts College, Tindivanam - 604 002. Tamil Nadu, India.
Email: srk.ss82@gmail.com[1]
Email: logeshkumaresan@yahoo.com[2]

Abstract- In the present investigation, Pure and dye (Sudan I) doped KDP crystals were grown by slow evaporation technique at room temperature. Grown crystals have been characterized using single crystal X-ray diffraction, Fourier Transform Infrared Spectroscopy (FTIR), UV- visible spectroscopy and NLO studies. The presences of dyes were confirmed by FTIR and XRD spectra. Dye molecules possess π electron similar to conjugated polymers, but the molecules themselves are not very big. The analysis of single crystal XRD spectra confirms that all the doped samples have the perfect crystal properties. Their energy level structure shows the presence of bands containing many closely spaced levels corresponding to vibrational and rotational states. A variety of dyes for many laser operating wavelengths were employed in the past. The dielectric behaviour of the pure and doped crystals conformed by LCRZ meter. The NLO reports of the samples are having high energy level comparing with pure KDP. Dyes embedded in KDP crystal and dye-doped crystals were also reported as useful non-linear optical media. The mechanical properties of the crystals were confirmed by Vicker's Microhardness Tester. Hence, the energy levels of the molecules are examined in HOMO-LUMO studies.

Keywords: XRD, FTIR, NLO, KDP, HOMO-LUMO

1. INTRODUCTION

KH_2PO_4 (KDP) crystal is widely used and thoroughly studied NLO crystals. The NLO and other premises of the crystal have been enhanced by doping of organic impurities. In the present investigation, pure and dye (Sudan I) doped KDP crystals were grown by slow evaporation technique at room temperature. Grown crystals have been characterized using single crystal X-ray diffraction and NLO studies. The presences of dyes were confirmed by Fourier Transform Infrared Spectroscopy (FTIR) and UV- visible spectra. From the dielectric studies, the behavior of pure and doped samples is analyzed. The samples are having high energy level comparing with pure KDP which is shown in NLO report. By Vicker's Microhardness, the mechanical property of the doped samples was tested at different load as 25g, 50g, and 100g. The energy transmissions of the molecules are well defined in HOMO-LUMO studies. Here, the dyes embedded in KDP crystal and dye-doped crystals were also reported as useful non-linear optical media.

2. EXPERIMENT

2.1. Crystal growth

Crystal growth is defined as it's an art of science and the subject of the growth of crystals is an interdisciplinary one which presents many professional fields; solid state physicists, mineralogists, crystallographers, physical chemists, mathematicians, chemical engineers etc. The growth of single crystals has been well developed over the years to reach the needs of basic research and applications. The crystals are anisotropic in nature. The electrical, mechanical, magnetic and optical properties can differ according to the position in which they were measured (Mullin 1993). Crystals are used for the electronic devices because the charge carriers are electrons and holes which can move freely.

Crystal growth techniques are generally classified into three categories; they are growing from solution, growth from vapor and growth from the melt. All the growth techniques have numerous variations, all materials cannot be grown by all the above three methods. In my present work, the organic dyes such as Sudan I, Methyl red and Evans blue were doped with KDP in 0.1% ratio and grow by slow evaporation technique at room temperature.

2.2.Solubility

It is prudent to study the solubility of the samples in a preferred solvent before proceeding for the crystal growth. Solubility must be moderate and should have a positive temperature gradient in a selected

solvent. The Solubility of the pure and doped KDP in water was studied gravimetrically. Here, the water is mostly used as a natural solvent. If the material is not dissolved in de-ionized water then organic solvents such as acetone, ethanol, methanol etc are used. The dopant Sudan-I was not dissolved in water. So we take acetone as a solvent and mixed with KDP solution.

2.3. Slow evaporation technique

In this technique, an excess of a given solute is established by utilizing the difference between the rates of evaporation of the solvent and the solute. A solution of the compound is prepared using a suitable solvent.

Unlike in the cooling method, in which the total mass of the system stays constant, the solvent evaporation technique, the solution loses particles, which are infirmly bound to other components and therefore the volume of the solution decreases. In almost all cases, the vapour pressure of the solvent above the solution is higher than the vapour pressure of the solute and therefore the solvent evaporates more rapidly and the solution becomes supersaturated (Petrov 1969). Usually, it is sufficient to permit the vapour formed above the solution to go freely to the atmosphere. This is a very simple and oldest technique of crystal growth.

Using the method of dissolving in distilled water the KDP salt was purified by repeated recrystallization. In a slightly under saturation condition the solution of KDP salt was prepared. The solution was stirred well for four hours constantly using magnetic stirrer still the salt has been dissolved in water. Then the prepared solution was transferred into two clean Petri dishes and kept for crystallization at room temperature in a quiet place.

A supersaturated solution of pure KDP and 0.1% of Sudan I (dopant is separately dissolved in acetone and added with pure KDP solution) doped KDP at room temperature was obtained by the constant stirring up to five hours and then filter the solution into beakers. Then the solution was transferred to a petri dish and it was kept away from dust. Hence, the slow evaporation method was employed for the entire growth process.

After completion of growth run, the good quality crystals were harvested. The photographs of grown pure KDP and Sudan I doped KDP crystal is shown in fig. 1(a) and 1(b).

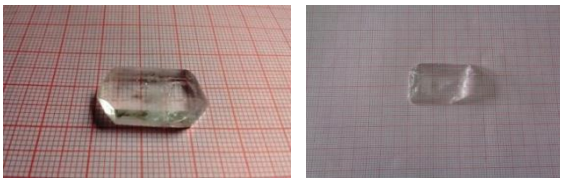

(a) (b)

Fig.1. 1(a) and 1(b) Pure KDP and Dyes doped KDP Crystals

3. CHARACTERIZATION

3.1. Single X-ray diffraction studies

The single crystal X-ray diffraction analysis has been carried out on the grown crystal. Single X-ray diffraction studies of pure and doped KDP crystals were carried out, using Bruker X8 Kappa ApeX11 XRD, X-ray diffractometer with Cu Kα (λ=1.54056Å) radiation. Fig.2. shows the unit cell determination of single crystal XRD pattern of the Pure and Sudan I doped KDP crystals. The diffraction patterns of the pure and dye-doped KDP have been indexed by the least square fit method. It is seen that both the pure and doped crystals crystallize variations in the lattice parameters which are due to the incorporation of the dopant in the KDP crystal lattice. From this spectral analysis, we conclude that the grown crystals all are having the properties of the crystals. This will show in table-1 the values of all doped samples having various crystal parameters (a, b, c) and the crystal system is tetragonal.

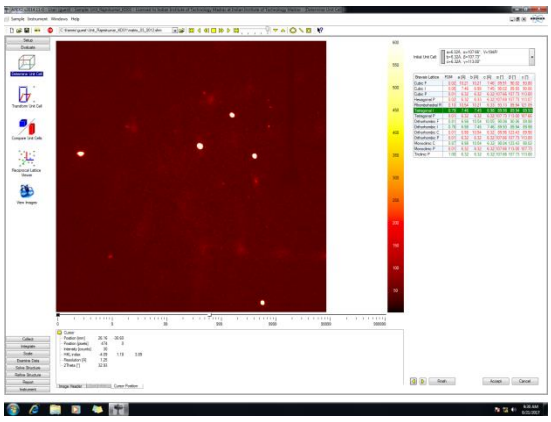

(a)

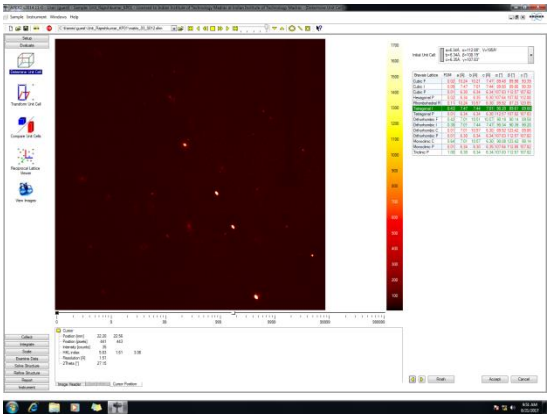

(b)

Fig.2. XRD of (a) Pure KDP and (b) Sudan I doped KDP Crystals

3.2. FTIR – Analysis

The FTIR (Fig.3) of all of them were recorded from solid phase samples on a Perkin Elmer- Spectrum 2 FTIR/ATR model spectrophotometer consists of globar and mercury vapor lamp as a source, an interferometer chamber having a comprising of KBr and Mylar beam splitters followed by a sample chamber and detector. An entire region of 4000 – 450 cm-1 is covered by this instrument. The instrument has a typical resolution of 0.5 cm-1. The infrared spectrum is useful in identifying the functional groups like –OH, -CN, -CO, -CH, -NH2, etc. Hence, the quantitative estimation is possible in certain cases for chemicals, pharmaceuticals, petroleum products, etc. From the below figure, it shows the graphical representation of the absorption spectrum of doped KDP samples. In the specified region of 510 cm-1 mostly all the samples having the maximum absorption ranges.

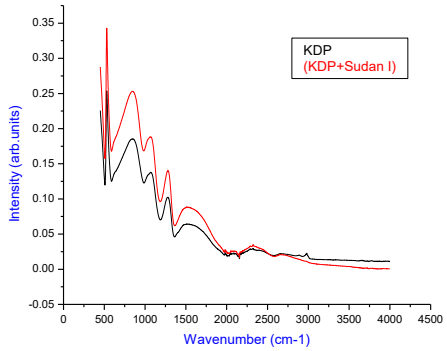

Fig.3. FTIR Spectra of (a) Pure KDP and (b) Sudan I doped KDP Crystals

3.3. UV – Visible Spectrum

The microprocessor was controlled this double-beam instrument. The instrument has bandwidth range 0.5 – 4 nm (variable). The spectrometer is well suited for samples both in solid and the dissolved form. The absorption spectrums for samples were measured over the wavelength range 200 nm to 900 nm. The graphs for absorption have been plotted in Fig.4. The pure and doped KDP crystals show a good absorption between 200 nm to 900 nm.

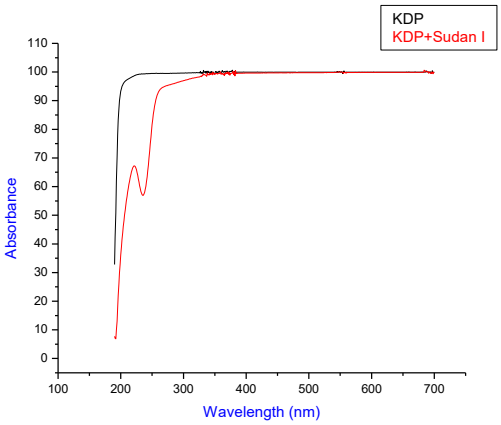

Fig.4. UV-Visible Spectra of (a) Pure KDP and (b) Sudan I doped KDP Crystal

3.4. NLO Analysis

The instruments specifications in Q switched High Energy of Nd: YAG Laser (Quanta ray Model LAB – 170 - 10) Model HG-4B- High efficiency, angle tuned and temperature stabilized Second harmonic and Third harmonic Generator Crystals. The Energy ranges are 850 mJ, 450 mJ & 220 mJ. The incident wavelength of the light is 1064 nm and the wavelength of the light emitted from the sample in this instrument is 532 nm. Instrument repetition rate was 10 Hz and the energy range is from 1.5 mJ to 3 J. The NLO reports of the samples are having high energy level comparing with pure KDP. The above table.2 shows variations and energy level difference in the pure and doped sample. Dyes embedded in KDP crystal and dye-doped crystal were also reported as useful non-linear optical media

3.5. *Homo-Lumo Analysis*

Complete geometrical optimizations of the investigated molecules are performed using DFT (density functional theory) with the Beck's three parameter exchange functional along with the Lee–Yang–Parr nonlocal correlation functional (B3LYP) [1] with 6-311++G(d,p) basis set is implemented in Gaussian 09 program package [2]. This approach is shown to yield favourable geometries for a wide

variety of systems. This basis set gives good geometry optimizations. The geometry structure was optimized under no constraint. The aim of our process is to calculate the following quantum chemical indices: The energy of highest occupied molecular orbital (EHOMO), the energy of lowest unoccupied molecular orbital (ELUMO), energy gap (ΔE) between EHOMO and ELUMO, dipole moment (μ), electronegativity (χ), electron affinity (A), global hardness (η), softness (σ), ionization potential (I), the global electrophilicity (ω), and the fraction of electrons transferred (ΔN) and correlate these with the experimental observations. The optimized structures of SUDAN 1 doped with KDP are depicted in Fig 5 which is shown below. Hence, the frontier orbital (highest occupied molecular orbital HOMO and lowest unoccupied molecular orbital LUMO) of a chemical species are very important in explaining its reactivity. Fukui first recognized this. A good correlation has been found between the speeds of corrosion and EHOMO that is often associated with the electron sharing ability of the molecule. Survey of literature shows that the adsorption of the inhibitor on the atom-surface can occur on the basis of donor-acceptor interactions between the π-electrons of the heterocyclic compound and the vacant d-orbital of the atom-surface atoms, high value of EHOMO of the molecules shows its tendency to donate electrons to appropriate acceptor molecules with low energy empty molecular orbitals. The increasing values of EHOMO facilitate adsorption and therefore enhance the inhibition efficiency, by influencing the transport process through the adsorbed layer. Where the similar relations were found between the rates of corrosion and ΔE (ΔE = ELUMO − EHOMO). When the energy of the lowest unoccupied molecular orbital indicates the ability of the molecule to accept electrons.

Here the lower value of ELUMO, the more probable the molecule would accept electrons. Consequently, concerning the value of the energy gap ΔE, larger values of the energy difference will give low reactivity to a chemical species. When the lower values of the ΔE will render good inhibition efficiency because the energy required removing an electron from the lowest occupied orbital will be low. From the EHOMO and ELUMO of the inhibitor, the molecule was related to the ionization potential (I) and the electron affinity (A), respectively. Then the ionization potential and the electron affinity are defined as I = - EHOMO and A = - ELUMO, respectively. Then the absolute electronegativity (χ) and global hardness (η) of the inhibitor molecule are approximated as follows:

$\chi = (I+A) / 2$

$\eta = (I-A) / 2$

The global electrophilicity index was introduced by Parr and is given by:

$\omega = \mu 2 / 2\eta$

The Quantum chemical parameters obtained from the calculations which are responsible for the inhibition efficiency of inhibitors, such as the highest occupied molecular orbital (EHOMO), energy of lowest unoccupied molecular orbital (ELUMO), HOMO–LUMO energy gap (ΔEH-L), dipole moment (μ) and total energy (TE), electronegativity (χ), electron affinity (A), global hardness (η), softness (σ), ionization potential (I), The global electrophilicity (ω), are collected in Table 3.

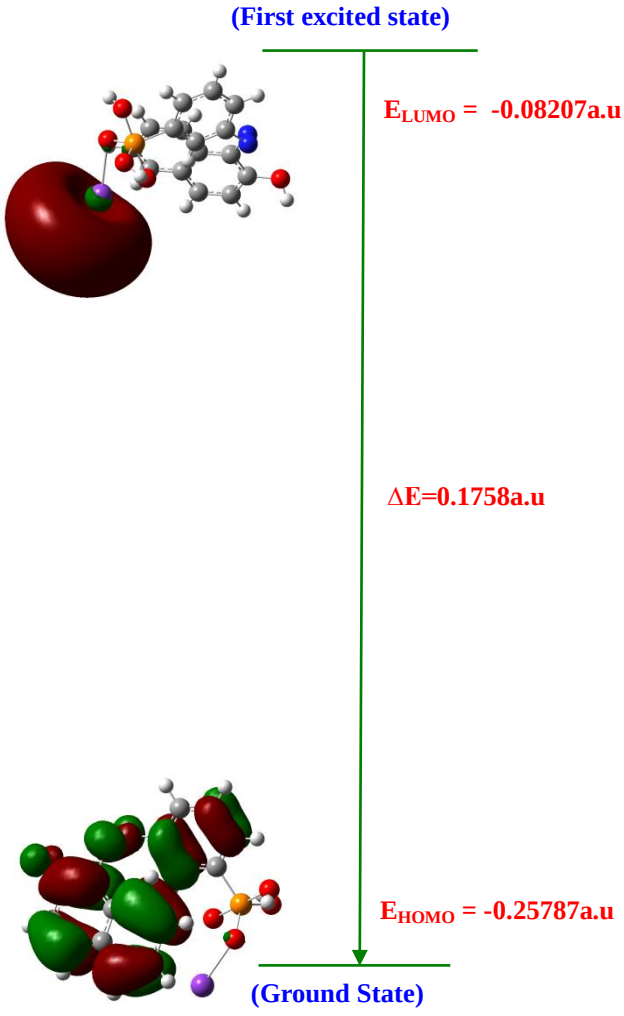

Fig.5.HOMO-LUMO Plot of Sudan I doped with KDP

3.6 Molecular electronic potential maps

The electrostatic potential is indicant for molecule charge distribution in three-dimensions. Indeed this map enables people to diagnose and investigate the distribution of atoms charge in the different parts of the molecule. However, the prediction of behaviour and performance of the molecule in chemical reactions could be done by this map [3]. For calculating and displaying this map, initially the related structure has been optimized using density functional theory and in the following the electrostatic potential map has been calculated and recorded by Molekel program. As this map, shows the modality of charge distribution for different parts of a molecule. The theoretical level of B3LYP, for electrophilic and nucleophilic reaction, is shown in Figs.6-8. Hydrogen atoms in this map have the minimum level of electrostatic potential and oxygen atoms have the maximum level of electrostatic potential. In addition, P atom is seen in green colour and is in the middle range of electrostatic potential level. In addition, nitrogen atoms related to the Naphthalene group is seen approximately yellow in the electrostatic potential map and approximately have more negative level than K atom.

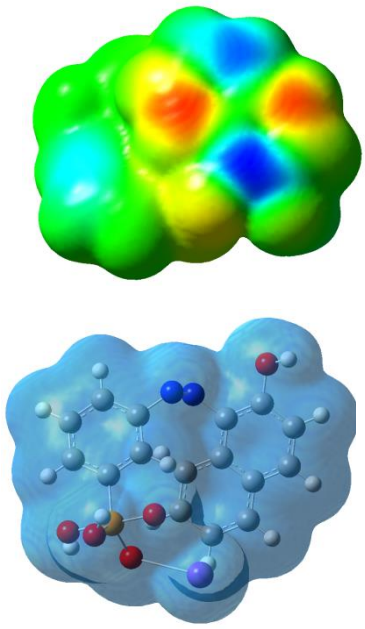

Fig.6.The molecular electrostatic potential surface density of SUDAN I doped with KDP.

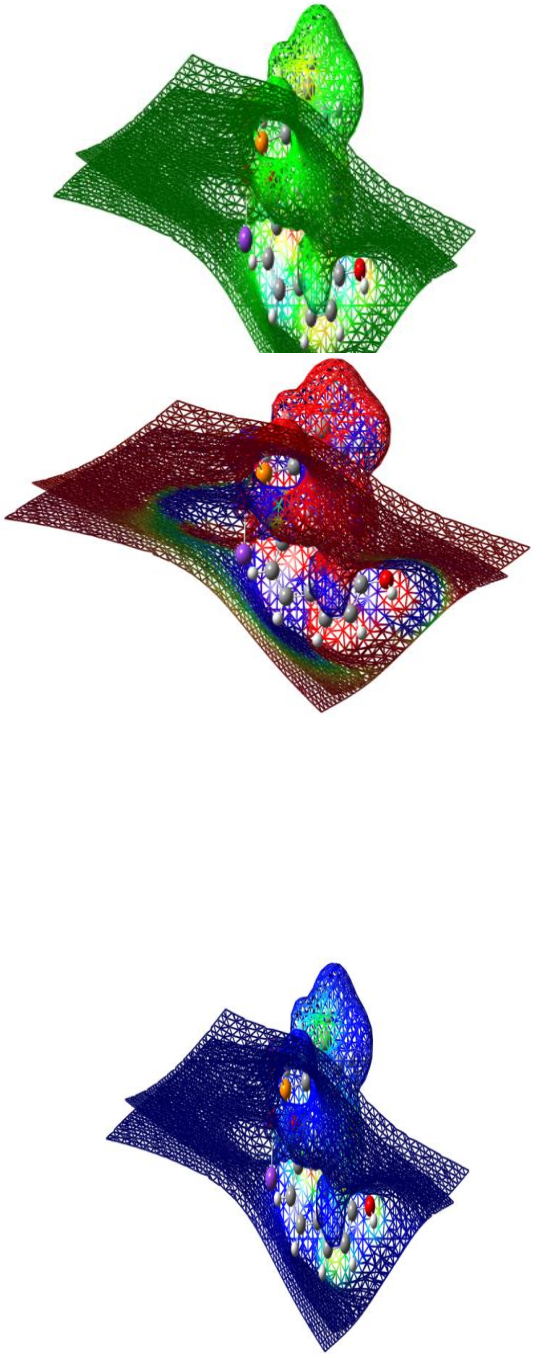

Fig.7.Different orientation of total electron of Sudan I

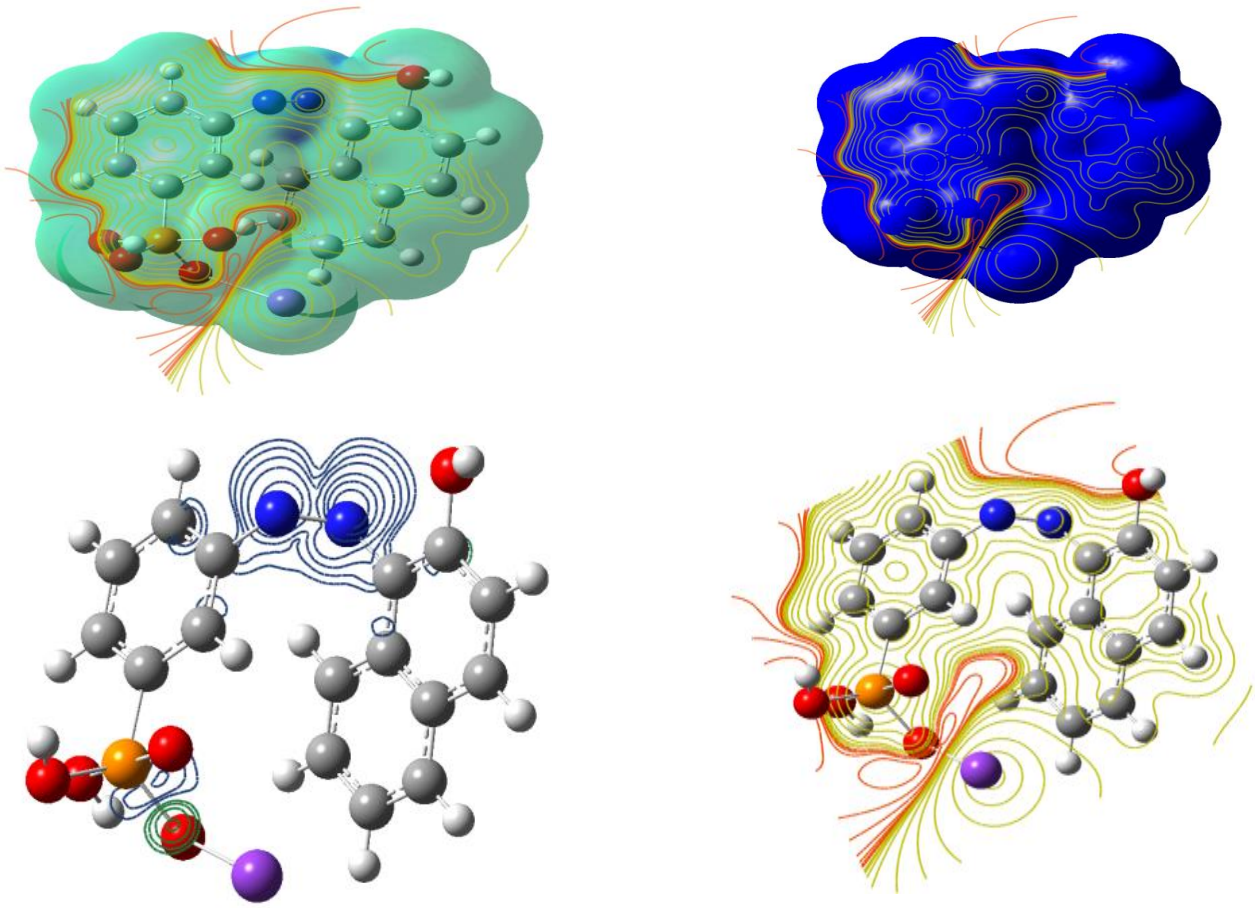

Fig.8.Different counter mapping surface of SUDAN I doped with KDP.

3.7. Microhardness measurements

The Sudan I doped KDP crystals were subjected to Vicker's static indentation test at room temperature using Shimadzu (Model HMV 2T) hardness tester. Loads of different magnitudes ranging from 25g – 100g were applied for the duration of 5 seconds. Vickers hardness (VHN) is given by the relation

$$\mathbf{H_v = 1.854\ P / d^2\ \ (Kilogram / millimetre^2)}$$

Where P is the test load in kg, d is the mean diagonal length of indentation in mm and 1.854 is a constant of a geometrical factor for the diamond pyramid. Generally, the hardness of the material varies with the applied load. The applied indentation test load is balanced by the total specimen resistance composed of four components due to: (1) friction at the indenter/specimen facet interface (frictional component), (2) elastic deformation, (3) plastic deformation, and (4) specimen cracking.

The plot of Vicker's hardness (VHN) versus load (P) for Sudan I doped KDP crystal is shown in below figure. It is seen from the figure that the hardness value increases with an increase in the doping concentration. Also with the increase in indenter load, the hardness increases.

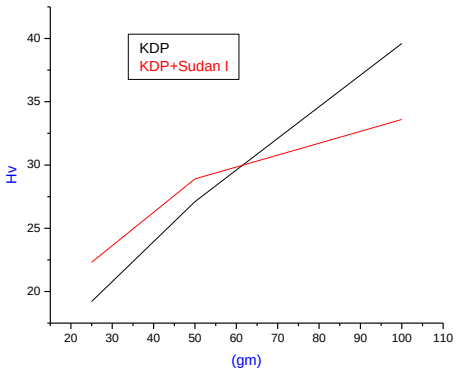

In the present work, microhardness of the pure and doped crystals is increased and reaches the saturation

around 100 g of load and beyond which the materials undergo cracks. From the analysis see that pure KDP curve has straight peak but the doped material has increased till 50g after that the hardness value decreasing as comparing with KDP. The mechanical properties of the doped crystal are increased compared with pure KDP crystals.

3.8. Dielectric studies

The dielectric study was carried out using LCRZ Meter unit in the frequency range of 50 Hz - 200 KHz. Figure-10 shows the plots of the dielectric constant (εr) and dielectric loss (tanδ) versus frequency for pure and Sudan I doped KDP crystals. In the lower frequency region, the dielectric constant and dielectric loss have high values. The dielectric constant and dielectric loss both decrease as the frequency increases and at high-frequency region both remain almost constant, which is a normal dielectric behaviour [38-43]. The relation of the dielectric constant (εr) was calculated by

$$\varepsilon r = [\, Cd / A\varepsilon o]$$

Where C is the capacitance value of the crystal, A is the area of the crystal under investigation, d is the thickness of the sample used and εo is the permittivity of free space.

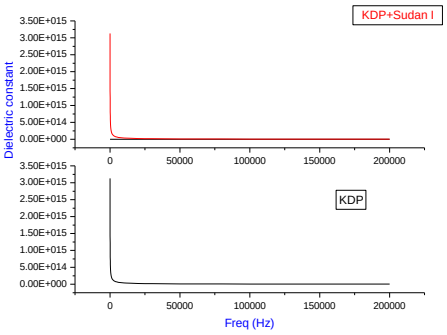

Fig.10. Dielectric constants for pure and doped KDP crystals

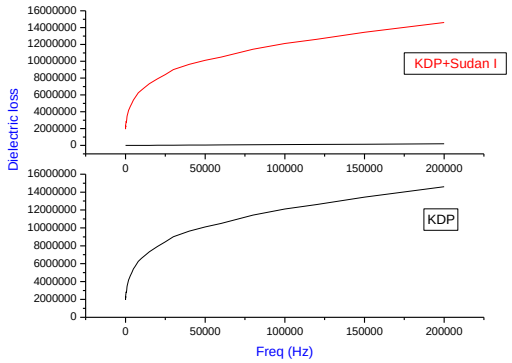

Fig.11.Dielectric losses for pure and doped KDP crystals

The loss tangent (tanδ) is a parameter of a dielectric material that quantifies its inherent dissipation of electromagnetic energy. The dielectric loss (ε") was given by

$$\varepsilon'' = \tan \delta\, \varepsilon r$$

The dielectric constant and the dielectric loss of Sudan I doped KDP crystals are lower than the pure KDP crystals.

4. RESULTS AND DISCUSSION

When Sudan I dye has been doped with KDP crystal it has some changes in its characteristics. By comparing pure KDP crystal the characteristic analysis in dye-doped KDP crystal has been studied by using single crystal XRD and NLO analysis. The excitation of X-ray in KDP doped crystals has been found. While comparing the XRD pattern of doped KDP crystals with pure KDP crystal structure the 2θ values slightly shifted towards left i.e. the 2θ values decreased infraction and hence the d-spacing range increased in the fraction. The pyramidal plane (110) and (101) has been dominated heavily whereas the basal plane (200) is unaffected. From FTIR pattern it was found that a strong absorption peak near the wavelength of 480nm in pure KDP crystal. Whereas in Sudan I dye-doped KDP crystal the absorbance range is shifted towards the higher wavelength side around 480nm. This implies that Sudan I dye finely incorporated in KDP crystal.

The NLO reports of the samples are having high energy level comparing with pure KDP. Dyes embedded in KDP crystal and dye-doped crystal were also reported as useful non-linear optical media. The aim of our calculation is to calculate the following quantum chemical indices in the HOMO-LUMO analysis. The energy of highest occupied molecular orbital (EHOMO), the energy of lowest unoccupied molecular orbital (ELUMO), energy gap (ΔE) between EHOMO and ELUMO, dipole moment (μ), electronegativity (χ), electron affinity (A), global hardness (η), softness (σ), ionization potential (I), the global electrophilicity (ω), and the fraction of electrons transferred (ΔN) and correlate these with the experimental observations. The chemical reaction is predicted by Molecular electronic potential maps.

The mechanical properties of the doped crystals are analysis made by Vicker's static indentation test at room temperature using Shimadzu (Model HMV 2T) hardness tester. The pure and doped crystals are increased and reach the saturation around 100 g of load and beyond which the materials undergo cracks. From this, we know that the mechanical properties of the doped crystal are increased compared with pure KDP crystals. From the dielectric studies the dielectric constant and dielectric loss both decrease as the frequency increases and at high-frequency region both

remain almost constant, which has a normal dielectric behaviour in the doped crystals.

5. CONCLUSION

Using FTIR and XRD analysis, the data Sudan I dye-doped KDP crystal has some changes in its structure. The shift of absorption and excellent transmission in the entire visible region makes this crystal a good candidate for electronic applications. In the NLO report, the samples are having high energy level comparing with pure KDP. From the HOMO-LUMO energy plot, we predict that the molecular energy levels are defined and calculated. Molecular electronic potential maps show the modality of charge distribution for different parts of the molecule. The mechanical properties of the doped crystals are determined by Vicker's hardness test and the hardness value increases with an increase in the doping concentration. In the dielectric studies, the dielectric constant and dielectric loss both decrease as the frequency increase as which is a normal dielectric behaviour. The characteristics study of grown Sudan I dye-doped KDP crystal indicated that this crystal can be a high NLO crystal than a pure KDP crystal. From this, we conclude that by comparing with KDP the doped crystals have high NLO properties. So the doped crystal has a major role in the non-linear optical fields.

Table: 1 – Unit cell Determination

MATERIALS	**CRYSTAL SYSTEM**	**UNIT CELL PARAMETERS**						
		a	**b**	**c**	**α**	**β**	**γ**	**V**
Pure KDP (KD01)	Tetragonal I	6.32	6.32	6.32	107.66	107.73	113	194
KDP + Sudan I (KP01)	Tetragonal I	6.34	6.34	6.35	112.88	108.19	109.83	195

Table: 2 – NLO Analysis

Sl. No.	Name of the sample	Output Energy (milli joule)	Input Energy (joule)
1	KDP	12.98	0.70
2	KDP+Sudan I	14.76	0.70

Table 3: HOMO- LUMO energy gap and related molecular properties of SUDAN 1 doped with KDP.

Molecular Properties	B3LYP/6-311++G(d,p)
HOMO	-0.25787 a.u
LUMO	-0.08207 a.u
Energy gap	0.1758 a.u
Ionization Potential (I)	0.25787 a.u
Electron affinity(A)	0.08207 a.u
Global softness(s)	11.3765 a.u
Global Hardness (η)	0.0879 a.u
Electro negativity (χ)	0.9668 a.u
Global Electrophilicity (ω)	-0.1642 a.u

REFERENCES

[1] G. Ramasamy and G.Bhagavannanarayanana, , Ind. J. Pure Appl. Phys. 52, 255(2014).
[2] G. G.Muley, Sci. Technol. 2, 109 (2012).
[3] G. G. Muley, M. N. Rode, and B. H. Pawar, Acta Polonica A 116, 1033 (2009).
[4] B. S. Kumar and K. R. Babu, Indian J. Pure Appl. Phys.46, 123 (2008).
[5] P. Kumaresan and S. Moorthy Babu J. Optoelectron. Advc. Mater. 9, 1299 (2007).
[6] P. Rajesh, P. Ramasamy, J. Cryst. Growth 311, 3491(2009).
[7] P. Rajesh and P. Ramasamy, Phys. B 404, 1611(2009).
[8] P.V.Dhanraj, C.K.Mahadevan, J.Cryst.Growth, 310,24(2008).
[9] Selemai Seif, Jiann Min Chang, Cryst.Growth Design, 1(5),pp 359-362,(2001).
[10] I.Pritula, A.Kosinova, Matrl.Resch.Bulletin, 43,10(2008).
[11] K.D.Parikh, D.J.Dave, Cryst.Resch.Tech,45,6(2010).
[12] Dave.D.J, Parikh.K.D,Optoelectronic & Adv.Matrl, 11, pp 602-609(2009).
[13] I.Pritula, O.Bezkrovnaya, Matrl.Che&Phy, 129, 777(2011).
[14] P.V.Dhanaraj, N.P.Rajesh, Condensed Matter, 404, 2503(2009).
[15] Mohd Anis, G.G.Mulley, Optical Materials, 46, 517(2015).
[16] Shivani Singh, Bansi Lal, J.Cryst.Growth, 312, 443(2010).
[17] R.Krishnamurthy, R.Rajasekaran, Molecular & Bio Molecular Spec. 104, 310(2013).
[18] Mohd Shakir, V.Ganesh, Int.J.Pure & A.Phy, 7, pp 13-24(2011).
[19] A.Kumaresh, B.Arun kumar, Molecular & Bio Molecular Spec.111, 179(2013).
[20] G.Ramasamy, S.P.Meenakshisundaram Ind. J. Pure Appl. Phys.122,pp 1121-1125(2013).
[21] B. Latha , P. Kumaresan, S. Nithiyanantham ,K. Sambathkumar J Molecular Structure 1152 (2018) 351-360
[22] K. Sambathkumar, S. Nithiyanantham, *J Mater Sci: Mater Electron* (2017),28, 6529–6543.
[23] K.Sambathkumar,S.Jeyavijayan,M.Arivazhagan *Spectrochim. Acta A* (2015). 147, 51-66.
[24] G. G. Muley, M. N. Rode, and B. H. Pawar, Acta Polonica A 116, 1033 (2009).
[25] B. S. Kumar and K. R. Babu, Indian J. Pure Appl. Phys.46, 123 (2008).
[26] P.Kumaresan and S. Moorthy Babu J. Optoelectron. Advc. Mater. 9, 1299 (2007).
[27] P. Rajesh, P. Ramasamy, J. Cryst. Growth 311, 3491(2009).
[28] G.Ramasamy and G. Bhagavannanarayanana, , Ind. J. Pure Appl. Phys. 52, 255(2014).
[29] G. G.Muley, Sci. Technol. 2, 109 (2012).
[30] P. Rajesh and P. Ramasamy, Phys. B 404, 1611(2009).
[31] Mohd Shakir, V.Ganesh, Int.J.Pure & A.Phy, 7, pp 13-24(2011).
[32] A.Kumaresh, B.Arun kumar, Molecular & Bio Molecular Spec.111, 179(2013).
[33] G.Ramasamy, S.P.Meenakshisundaram Ind. J. Pure Appl. Phys.122,pp 1121-1125(2013).
[34] Pritula, A.Kosinova, Matrl.Res.Bulletin. 43 (2008) 2778-2789.
[35] J.Podder, S.Ramalingom, Crys.Res.Technol. 36 (2006) 549-556.
[36] I.Pritula, A.Kosinova, Funct.Matrl. 14 No.3 (2007).
[37] Dave.D.J, Parikh.K.D,Optoelectronic & Adv.Matrl, 11, pp 602-609(2009).
[38] I.Pritula, O.Bezkrovnaya, Matrl.Che&Phy, 129, 777(2011).
[39] P.V.Dhanaraj, N.P.Rajesh, Condensed Matter, 404, 2503(2009).
[40] Mohd Anis, G.G.Mulley, Optical Materials, 46, 517(2015).
[41] Shivani Singh, Bansi Lal, J.Cryst.Growth, 312, 443(2010).
[42] P.V.Dhanraj, C.K.Mahadevan, J.Cryst.Growth, 310,24(2008).
[43] Selemai Seif, Jiann Min Chang, Cryst.Growth Design, 1(5),pp 359-362,(2001)
[44] A.Bensouici, J.L.Plaza, Jounl.of Opt Elec. Vol.10, No.11, (2008), 3051-3053.
[45] S.Javidi, M.Esmaeil Nia, Semi.con Phy Vol.11, No.4, 342-344 (2008).
[46] Z.Delci, D.Shyamala, Int.Nat J. Chem Res. Vol.4, No.2, 816-826 (2012).
[47] I.Pritula, A.Kosinova, Matrl.Resch.Bulletin, 43,10(2008).
[48] K.D.Parikh, D.J.Dave, Cryst.Resch.Tech,45,6(2010).
[49] B. Latha , P. Kumaresan, S. Nithiyanantham , K. Sambathkumar Journal of Molecular Structure 1142 (2017) 255-260
[50] M. Oftadeh, S. Naseh and M. Hamadanian, Computational and theoretical chemistry,
[51] *Chemical Physics Letters*, 966(2011), 20-25
[52] Sambathkumar, S. Nithiyanantham, Synthesis, characterization and theoretical properties of coumarin NLO single crystal by DFT method *J Mater Sci: Mater Electron* 2017,28, 6529–6543
[53] K.Sambathkumar, S.Jeyavijayan, M. Arivazhagan; Electronic structure investtigations of 4 aminophthal hydrazide by

UV–visible, NMR spectral studies and HOMO–LUMO analysis by ab initio and DFT calculations Spectrochim. Acta A 147 (2015)51-66.

[54] Keresztury G, Raman spectroscopy theory, in: JM Chalmers, P, Griffiths R (Eds.), Handbook of Vibrational Spectroscopy, Vol. 1, John Wiley & Sons Ltd., 2002, p. 71.

[55] http://riodbol.ibase.aist.go.jp/sdbs/(National Institute of Advanced Industrial Science).

[56] B. Latha , P. Kumaresan, S. Nithiyanantham ,K. Sambathkumar J Molecular Structur 1152 (2018) 351-360

[57] K. Sambathkumar, S. Nithiyanantham, *J Mater Sci: Mater Electron* (2017),28, 6529–6543.

[58] K.Sambathkumar,S.Jeyavijayan,M.Arivazhagan *Spectrochim. Acta A* (2015). 147, 51-66.